ISSN 1674-1056
http://cpb.iphy.ac.cn
http://iopscience.iop.org/cpb
中国物理 B
Chinese Physics
中国物理
Chinese Physics B

Explicitly correlated configuration interaction investigation on low-lying states of SiO^+ and SiO

Rui Li(李瑞), Gui-Ying Liang(梁桂颖), Xiao-He Lin(林晓贺), Yu-Hao Zhu(朱宇豪), Shu-Tao Zhao(赵书涛), Yong Wu(吴勇)

Citation: Chin. Phys. B . 2019, 28(4): 043102. **doi:** 10.1088/1674-1056/28/4/043102
Journal homepage: http://cpb.iphy.ac.cn; http://iopscience.iop.org/cpb

What follows is a list of articles you may be interested in

Theoretical study of spin-forbidden cooling transitions of indium hydride using *ab initio* methods

Yun-Guang Zhang(张云光), Hua Zhang(张华), Ge Dou(窦戈)
Chin. Phys. B . 2017, 26(9): 093101. **doi:** 10.1088/1674-1056/26/9/093101

Potential energy curves, transition dipole moments, and radiative lifetimes of KBe molecule

Ming-Jie Wan(万明杰), Cheng-Guo Jin(金成国), You Yu(虞游), Duo-Hui Huang(黄多辉), Ju-Xiang Shao(邵菊香)
Chin. Phys. B . 2017, 26(3): 033101. **doi:** 10.1088/1674-1056/26/3/033101

Low-lying electronic states of CuN calculated by MRCI method

Shu-Dong Zhang(张树东), Chao Liu(刘超)
Chin. Phys. B . 2016, 25(10): 103103. **doi:** 10.1088/1674-1056/25/10/103103

Spectroscopic properties and radiative lifetimes of SiTe：A high-level multireference configuration interaction investigation

Li Rui, Zhang Xiao-Mei, Jin Ming-Xing, Xu Hai-Feng, Yan Bing
Chin. Phys. B . 2014, 23(5): 053101. **doi:** 10.1088/1674-1056/23/5/053101

Multireference calculations on low-lying states and $X^3\Pi_u$-$^3\Pi_g$ absorption spectra of indium dimer

Zhou Ling-Song, Yan Bing, Jin Ming-Xing
Chin. Phys. B . 2013, 22(4): 043102. **doi:** 10.1088/1674-1056/22/4/043102

Explicitly correlated configuration interaction investigation on low-lying states of SiO^+ and SiO*

Rui Li(李瑞)[1,2,†], Gui-Ying Liang(梁桂颖)[2], Xiao-He Lin(林晓贺)[2], Yu-Hao Zhu(朱宇豪)[2], Shu-Tao Zhao(赵书涛)[3], and Yong Wu(吴勇)[2,4,‡]

[1] *Department of Physics, College of Science, Qiqihar University, Qiqihar* 161006, *China*
[2] *Institute of Applied Physics and Computational Mathematics, Beijing* 100088, *China*
[3] *School of Physics and Electronic Science, Fuyang Normal University, Fuyang* 236037, *China*
[4] *HEDPS, Center for Applied Physics and Technology, Peking University, Beijing* 100084, *China*

(Received 12 December 2018; revised manuscript received 29 January 2019; published online 5 March 2019)

SiO^+ and SiO, which play vital roles in astrophysics and astrochemistry, have long attracted considerable attention. However, accurate information about excited states of SiO^+ is still limited. In this work, the structures of 14 Λ–S states and 30 Ω states of SiO^+ are computed with explicitly correlated configuration interaction method. On the basis of the calculated potential energy curves of those Λ–S states and Ω states, the spectroscopic constants of bound states are evaluated, which are in good agreement with the latest experimental results. The predissociation mechanism of $B^2\Sigma^+$ state is illuminated with the aid of spin–orbit coupling matrix elements. On the basis of the calculated potential energy curves and transition dipole moments, the radiative lifetime for each of low-lying vibrational states $B^2\Sigma^+$ and $A^2\Pi$ is estimated. The laser cooling scheme of SiO^+ is proposed by employing $B^2\Sigma^+$–$X^2\Sigma^+$ transition. Finally, the vertical ionization energy values from SiO ($X^1\Sigma^+$) to ionic states: SiO^+, $X^2\Sigma^+$, $B^2\Sigma^+$, and $A^2\Pi$ are calculated, which agree well with experimental measurements.

Keywords: SiO^+, explicitly correlated configuration interaction, transition dipole moment, ionization energy

PACS: 31.50.Df, 31.15.aj, 31.15.ag **DOI:** 10.1088/1674-1056/28/4/043102

1. Introduction

SiO^+ and SiO play important roles in astrophysics and astrochemistry, which have been photographed in hot circumstellar regions,[1,2] interstellar clouds,[3–8] meteor emission.[9] The SiO^+ cation was also readily generated by shock-heated dense molecular clouds.[10,11] In order to illuminate the physical and chemical phenomenons of SiO^+ in celestial body, it is necessary to study the electronic structures and spectroscopic properties of the ion. In recent years, SiO^+ has also aroused growing interest in scientific research due to the application in the laser cooling of molecular ions.[12] The accurate control of internal and external degree of laser cooling molecular ion has potential applications in metrology, quantum information, and quantum computation.[13–16] Stollenwerk *et al.*[12] obtained a trapped sample of SiO^+ by employing supersonic expansion. The transition dipole moment and radiative lifetime of $B^2\Sigma^+$–$X^2\Sigma^+$ transition were investigated in detail. Apart from $B^2\Sigma^+$ state, the other low-lying states $X^2\Sigma^+$ and $A^2\Pi$ have been studied by Rosner *et al.*[17–21] through utilizing the approach of fast-ion beam, and the interaction and rotation vibration spectra of the two low-lying states were analyzed in detail. The spectroscopic constant for each of $X^2\Sigma^+$, $A^2\Pi$, and $B^2\Sigma^+$ was evaluated in their investigations, and fine-structure constant of $X^2\Sigma^+$ was obtained from the high-resolution spectrum.

Along with experimental investigations, a series of theoretical studies have been carried out to study the electronic structures and spectroscopic properties of the low-lying states of SiO^+. In 1978, Colbourn *et al.*[22] used multiple-scattering X_α transition-state method to determine the vertical ionization potential for each of $X^2\Sigma^+$, $A^2\Pi$, and $B^2\Sigma^+$ of SiO^+ relative to the ground state $X^1\Sigma^+$ of SiO. Later, Werner *et al.* used the multiconfiguration self-consistent field (MCSCF) method to calculate the potential energy curves (PECs) and dipole moment (DM) curves of $X^2\Sigma^+/A^2\Pi$ of SiO^+,[23] which predicted the ion to be a good IR emitter. Cai and François[24] studied the electronic structures of the low-lying states associated with the two lowest dissociation limits, and gave the spin-allowed transition dipole moments and radiative lifetimes for the three low-lying vibrational levels of $B^2\Sigma^+$. Nguyen and Odom[25] utilized the calculated PEC and transition probability for each of $B^2\Sigma^+$–$X^2\Sigma^+$, $A^2\Pi$–$X^2\Sigma^+$, $B^2\Sigma^+$–$A^2\Pi$ to simulate laser cooling scheme of SiO^+. Chattopadhyaya *et al.*[26] adopted the relativistic configuration interaction method to investigate

*Project supported by the National Key Research and Development Program of China (Grant No. 2017YFA0402300), the Science Challenge Project (Grant No. TZ2016005), the China Postdoctoral Science Foundation (Grant No. 2018M631404), the National Natural Science Foundation of China (Grant No. 11404180), the University Nursing Program for Yong Scholars with Creative Talents in Heilongjiang Province, China (Grant No. UNPYSCT-2015095), the Natural Science Research Project of Education Department of Anhui Province, China (Grant No. KJ2018A0342), and the Key Program of Excellent Youth Talent Project of Fuyang Normal University, China (Grant No. rcxm201801).

†Corresponding author. E-mail: lirei01@163.com

‡Corresponding author. E-mail: wu_yong@iapcm.ac.cn

© 2019 Chinese Physical Society and IOP Publishing Ltd

the electronic spectrum of SiO^+ within 7 eV. The spectroscopic constants of six low-lying Ω states ($X^2\Sigma^+_{1/2}$, $A^2\Pi_{3/2}$, $A^2\Pi_{1/2}$, $B^2\Sigma^+_{1/2}$, $1^4\Sigma^+_{1/2}$, and $1^4\Sigma+3/2$) were obtained in their calculations. However, the previous theoretical investigations only considered the spin–orbit coupling (SOC) of the four low-lying states ($X^2\Sigma^+$, $A^2\Pi$, $X^2\Sigma^+$, and $1^4\Sigma^+$), and the spectroscopic properties of low-lying states affected by SOC effect have been still unclear.

In this work, we use the high-level *ab initio* method to calculate the low-lying electronic states of SiO^+. The PECs of 14 Λ–S states and 30 Ω states are determined by the theoretical calculation. In the SOC calculation, the coupling effects of the 14 Λ–S states are simultaneously taken into account. Based on the computed PECs, the spectroscopic constant for each of bound Λ–S and Ω state is evaluated by the numerical method. Based on the calculated PECs and transition dipole moments, the radiative lifetimes of several low-lying vibrational states of $B^2\Sigma^+$ and $A^2\Pi$ electronic states are computed. On the basis of $B^2\Sigma^+$–$X^2\Sigma^+$ transition, the feasibility of laser cooling of SiO^+ is discussed. Finally, the vertical ionization energy values from SiO ($X^1\Sigma^+$) to several ionic states of SiO^+ are determined.

2. Methods and computational details

In the present work, the accurate electronic structure of SiO^+ is computed with MOLPRO 2012 suite of quantum chemical program.[27] Owing to the limit of MOLPRO program, the Abel point group C_{2v} is applied, and the low-lying electronic states of SiO^+ are expressed as follows: $\Sigma^+ = A_1$, $\Sigma^- = A_2$, $\Pi = B_1 + B_2$, and $\Delta = A_1 + A_2$. For Si and O, the Gaussian-type all-electron basis sets cc-pVQZ-F12 are selected.[28] To obtain the accurate single point energy of electronic state, the electronic structure calculation is performed by the three steps below. First, Hartree–Fock (HF) method is used to compute the singlet-configuration wavefunction of the ground state. Second, utilizing the HF wavefunction as the initial guess, a multi-reference wavefunction is generated by the state-averaged complete active space self-consistent field (SA-CASSCF) computation.[29,30] Finally, utilizing the CASSCF wavefunction as reference, the singlet point energy values of Λ–S states are computed by the explicitly correlated multireference configuration interaction method (MRCI-F12).[31] The construction of active space in the CASSCF computation is crucial for the precision of electronic structure. We test different active spaces, and finally select 8 molecular orbitals (MOs) as active space. The 8 MOs, which correspond to the 3s, 4s, p_x, $3p_y$, $3p_z$ atomic orbitals of Si^+ and $2p_x$, $2p_y$, $2p_z$ atomic orbitals of O, are referred to as (9e,8o). In the following MRCI-F12 computation, the $1s^22s^22p^6$ electrons of Si^+ and $1s^2$ electrons of O are set to be core orbitals, while $2s^22p^1$ electrons of Si^+ and $2s^22p^4$ electrons of O are correlated with single and double excitations. In order to overcome the size-inconsistency problem caused by the MRCI-F12 method, the Davidson correction is taken into consideration.

To improve the precision of our calculation, the SOC effect of electronic states is considered as a perturbation via a two-step procedure.[32,33] The values of SO matrices are extracted from the SOC calculation.[34] The off-diagonal SO matrix elements are generated by the MRCI-F12 wave function, while the diagonal SO matrix elements are obtained from the MRCI-F12+Q computation. The PECs of Λ–S states and Ω states are plotted by connecting the energy points of low-lying states with the aid of the avoided crossing principle.

Based on the computed PECs, the spectroscopic constants, vibrational energy levels, vibrational wavefunctions and Franck–Condon factors (FCFs) of SiO^+ are given by the numerical solution of nuclear Schrödinger equation through employing LEVEL procedure.[35] The transition dipole moments are determined at the MRCI-F12 level in theory. On the basis of the computed transition dipole moments, energy gaps of vibrational levels, and FCFs, the radiative lifetime of $B^2\Sigma^+$ and $A^2\Pi$ state are estimated.

3. Results and discussion

3.1. Electronic structures and spectroscopic properties of Λ–S states

The 14 Λ–S states associated with the two lowest dissociation limits ($Si^+(^2P_u)+O(^3P_g)$) and ($Si^+(^2P_u)+O(^1D_g)$) are computed at MRCI-F12 level by employing the cc-pVQZ-F12 basis sets. The adiabatic PECs of the 14 Λ–S are presented in Fig. 1, which are constructed by 29 singlet point energy values in an internuclear distance range of 1.3 Å–3.5 Å.

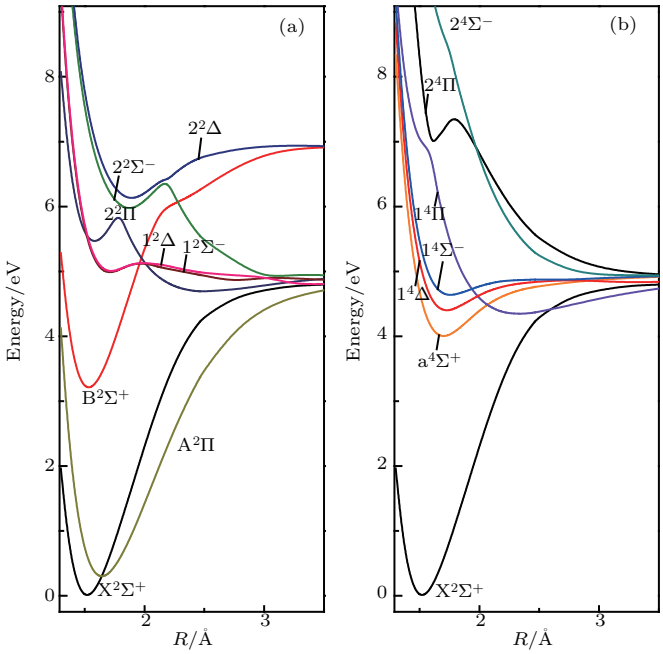


Fig. 1. Potential energy curves of (a) doublet Λ–S states of SiO^+ and (b) quartet Λ–S states of SiO^+.

Table 1. Spectroscopic constants of bound Λ–S states of SiO^+.

State		T_e/cm^{-1}	ω_e/cm^{-1}	$\omega_e x_e$/cm^{-1}	B_e/cm^{-1}	R_e/Å	Configuration at R_e/%
							$6\sigma^2 7\sigma^1 8\sigma^0 9\sigma^0 2\pi^4 3\pi^0 4\pi^0(73)$
$X^2\Sigma^+$		0	1159	7.4	0.7183	1.519	$6\sigma^1 7\sigma^2 8\sigma^0 9\sigma^0 2\pi^4 3\pi^0 4\pi^0(9)$
							$6\sigma^2 7\sigma^1 8\sigma^0 9\sigma^0 2\pi^3 3\pi^1 4\pi^0(9)$
	expt.[a]				0.7178	1.519	
	expt.[b]		1120			1.512	
	expt.[c]		1164		0.71762		
	expt.[d]				0.7325		
	expt.[e]		1162	6.8718	0.72055	1.516	
	Calc.[f]		1125			1.538	
	Calc.[g]		1166.9	8.15	0.70785	1.5295	
$A^2\Pi$		2397	929	4.9	0.6150	1.641	$6\sigma^2 7\sigma^2 8\sigma^0 9\sigma^0 2\pi^3 3\pi^0 4\pi^0(92)$
	expt.[b]	887	1030			1.645	
	expt.[e]	2242	944	5.0	0.6189	1.636	
	calc.[f]	790	923			1.656	
	Calc.[g]	1879	933.2	5.93		1.6443	
	Calc.[h]	2313	945.6		0.61685	1.6388	
							$6\sigma^1 7\sigma^2 8\sigma^0 9\sigma^0 2\pi^4 3\pi^0 4\pi^0(63)$
$B^2\Sigma^+$		25828	1121	6.4	0.7065	1.531	$6\sigma^2 7\sigma^1 8\sigma^0 9\sigma^0 2\pi^3 3\pi^1 4\pi^0(25)$
	expt.[a]				0.7103	1.527[a]	
	expt.[b]	25740	1180			1.545	
	expt.[c]	26017	1138		0.71076		
	expt.[e]	26016	1137	6.9202	0.71302		
	expt.[h]	26030					
	calc.[f]	25484	1107			1.546	
	Calc.[g]	25722	1124.7	7.22	0.69945	1.5391	
$1^2\Sigma^-$		40261	676	47.6	0.5771	1.707	$6\sigma^2 7\sigma^1 8\sigma^0 9\sigma^0 2\pi^3 3\pi^1 4\pi^0(92)$
	Calc.[f]	39611	522			1.776	
	Calc.[g]	40760	507.8		0.53112	1.728	
$1^2\Delta$		40401	856	153.1	0.5692	1.716	$6\sigma^2 7\sigma^1 8\sigma^0 9\sigma^0 2\pi^3 3\pi^1 4\pi^0(92)$
	Calc.[f]	39530	538			1.764	
	Calc.[g]	40785	561.1		0.53933	1.7319	
							$6\sigma^2 7\sigma^0 8\sigma^0 9\sigma^0 2\pi^4 3\pi^1 4\pi^0(62)$
$2^2\Pi$		44077	1096	60.4	0.6639	1.580	$6\sigma^1 7\sigma^1 8\sigma^0 9\sigma^0 2\pi^4 3\pi^1 4\pi^0(6)$
							$6\sigma^1 7\sigma^1 8\sigma^0 9\sigma^0 2\pi^4 3\pi^1 4\pi^0(3)$
							$6\sigma^2 7\sigma^0 8\sigma^0 9\sigma^0 2\pi^3 3\pi^2 4\pi^0(2)$
	Calc.[f]	44731	917			1.604	
	Calc.[g]	44680	913.2	15.13	0.66698	1.5768	
$2^2\Sigma^-$		48219	685	12.3	0.4726	1.873	$6\sigma^2 7\sigma^1 8\sigma^0 9\sigma^0 2\pi^3 3\pi^1 4\pi^0(87)$
	Calc.[f]	39530	538			1.764	
	Calc.[g]	49275	643.4	11.13	0.45935	1.8989	
							$6\sigma^2 7\sigma^1 8\sigma^0 9\sigma^0 2\pi^3 3\pi^1 4\pi^0(69)$
$2^2\Delta$		48336	572	8.4	0.4789	1.846	$6\sigma^1 7\sigma^2 8\sigma^0 9\sigma^0 2\pi^4 3\pi^0 4\pi^0(11)$
							$6\sigma^2 7\sigma^0 8\sigma^0 9\sigma^0 2\pi^4 3\pi^0 4\pi^0(5)$
							$6\sigma^2 7\sigma^1 8\sigma^0 9\sigma^0 2\pi^4 3\pi^0 4\pi^0(4)$
	Calc.[f]	47198	615			1.881	
	Calc.[g]	48229	577.5	7.13	0.4682	1.881	
$a^4\Sigma^+$		32289	767	20.6	0.5738	1.700	$6\sigma^2 7\sigma^1 8\sigma^0 9\sigma^0 2\pi^3 3\pi^1 4\pi^0(93)$
	Calc.[f]	30493	673			1.727	
	Calc.[g]	31984	712	15.37	0.56581	1.710	
$1^4\Delta$		35780	632	26.5	0.5574	1.727	$6\sigma^2 7\sigma^1 8\sigma^0 9\sigma^0 2\pi^3 3\pi^1 4\pi^0(94)$
	Calc.[f]	33957	547			1.768	
	Calc.[g]	35391	572.6	12.77	0.54337	1.7451	
$1^4\Sigma^-$		37447	463	23.5	0.5394	1.754	$6\sigma^2 7\sigma^1 8\sigma^0 9\sigma^0 2\pi^3 3\pi^1 4\pi^0(94)$
	Calc.[f]	35574	439			1.823	
	Calc.[g]	37277	460	22.05	0.51788	1.7893	
$1^4\Pi$		35136	265	3.9	0.3055	2.329	$6\sigma^1 7\sigma^1 8\sigma^0 9\sigma^0 2\pi^4 3\pi^1 4\pi^0(93)$
	Calc.[f]	30650	284			2.454	
	Calc.[g]	33959	301.6	5.71	0.29078	2.3841	
$2^4\Pi$		55939	2601		0.6487	1.608	$6\sigma^2 7\sigma^2 8\sigma^0 9\sigma^0 2\pi^2 3\pi^1 4\pi^0(86)$
	Calc.[f]	55548	908			1.587	
	Calc.[g]	55692	1453		0.59279	1.671	

[a]Ref. [36]. [b]Ref. [22], [c]Ref. [37], [d]Ref. [38], [e]Ref. [17], [f]Ref. [26], [h]Ref. [12], [g]Ref. [24].

From the PECs of Fig. 1, it can be seen that most of Λ–S states are typical bound states except for $2^2\Pi$, $1^4\Pi$, $2^4\Pi$, and $2^4\Sigma^-$. The shoulder in PEC of $2^2\Pi$ may be attributed to the avoided crossing phenomenon with $3^2\Pi$ state. The $1^4\Pi$ and $2^4\Pi$ form an avoided crossing point around $R = 1.6$ Å, leading to the irregular shapes of PECs of the $^4\Pi$ sates. On the basis of these calculated PECs, the spectroscopic constants of bound states are determined by numerical method and given in Table 1. The dominant electronic configurations of bound states at equilibrium distance are also listed in Table 1.

For the SiO^+ molecular ion, the dominated electronic state of the ground state $X^2\Sigma^+$ and the first excited state $A^2\Pi$ states are $6\sigma^2 7\sigma^1 8\sigma^0 9\sigma^0 2\pi^4 3\pi^0 4\pi^0$ (73%) and $6\sigma^2 7\sigma^2 8\sigma^0 9\sigma^0 2\pi^3 3\pi^0 4\pi^0$ (92%), respectively, which means that the $X^2\Sigma^+ \rightarrow A^2\Pi$ transition corresponds to the one electron promotion $2\pi \rightarrow 7\sigma$. Compared with previous results, our MRCI-F12 calculated results R_e (1.519 Å) and ω_e (1159 cm^{-1}) of $X^2\Sigma^+$ are close to the experimental results (1.516 Å and 1162 cm^{-1} [17]). For the spectroscopic constant of $A^2\Pi$ state, the T_e is calculated to be 2397 cm^{-1}, which is in good accordance with experimental value of 2242 cm^{-1}.[17] The calculated R_e is 1.641 Å, fitting very well with 1.645 Å derived from the photoelectron spectrum of SiO.[22] The calculated ω_e value of 929 cm^{-1} is in good agreement with the experimental result 944 cm^{-1} determined from the analysis of the two band systems $B^2\Sigma^+$–$A^2\Pi$ and $B^2\Sigma^+$–$X^2\Sigma^+$,[17] and is somewhat smaller than the predicted value 1030 cm^{-1} obtained from the photoelectron spectrum.[22]

Since the $B^2\Sigma^+$–$X^2\Sigma^+$ transition plays an important role in laser-cooling investigation of SiO^+,[12] the $B^2\Sigma^+$–$X^2\Sigma^+$ transition is well studied theoretically and experimentally. The dominated electronic states of $B^2\Sigma^+$ are $6\sigma^1 7\sigma^2 8\sigma^0 9\sigma^0 2\pi^4 3\pi^0 4\pi^0$ (63%) and $6\sigma^2 7\sigma^1 8\sigma^0 9\sigma^0 2\pi^3 3\pi^1 4\pi^0$ (25%), corresponding to $6\sigma \rightarrow 7\sigma$ and $2\pi \rightarrow 3\pi$ singlet electron transition relative to the $X^2\Sigma^+$ state. The computed values of B_e and R_e of $B^2\Sigma^+$ are 0.7065 cm^{-1} and 1.531 Å, which only differ from the experimental value by 0.0038 cm^{-1} and 0.004 Å, respectively.[36] The T_e values of $B^2\Sigma^+$ is computed to be 25828 cm^{-1}, which is closer to the recently experimental value of 26030 cm^{-1}, than to previous theoretical values of 25484[26] and 25722 cm^{-1}.[24] For the other bound states, our present spectroscopic constants are consistent with the theoretical values calculated recently at the CI and coupled cluster (CCSD(T)) level of theory,[24,26] which can motivate the future experiment to verify the correctness of these predictions.

3.2. Transition properties and scheme for laser cooling of SiO^+

The spin-allowed transition dipole moments $B^2\Sigma^+$–$X^2\Sigma^+$ and $A^2\Pi$–$X^2\Sigma^+$ transitions of SiO^+ are calculated with the MRCI-F12 method. In the Franck–Condon region, the averaged transition dipole moments of $B^2\Sigma^+$–$X^2\Sigma^+$ and $A^2\Pi$–$X^2\Sigma^+$ have large values, which are about 0.65 a.u. and 0.21 a.u. (the unit a.u. is short for atomic unit), respectively. Our theoretical values of the transition dipole moments of these two transitions are close to the recent experimental values of 0.64 a.u. and 0.08 a.u.[12] On the basis of the calculated PECs of Λ–S states, FCFs and transition dipole moments, the lifetime of low-lying vibrational state of bound state is determined by the following formula:

$$\tau = (\sum_{v''} A_{v'v''})^{-1}, \tag{1}$$

where Einstein coefficient $A_{v'v''}$ is determined by

$$A_{v'v''} = 2.026 \times 10^{-6} \Delta E (TDM)^2 q_{v'v''}. \tag{2}$$

In formulas (1) and (2), the unit of $A_{v'v''}$ is in unit of s^{-1}, the unit of energy gap ΔE is in unit of cm^{-1}, the unit of transition dipole moment (TDM) is a.u. Vibrational branching ratio $R_{v'v''}$ is determined from $R_{v'v''} = A_{v'v''} / \sum_{v''} A_{v'v''}$.

Oscillator strength $f_{v'v''}$ is evaluated from the FCFs and TDM by

$$f_{v'v''} = \frac{2}{3} \times \Delta E \times TDM^2 \times q_{v'v''}, \tag{3}$$

where ΔE and TDM are in atomic unit.

According to formulas (1) and (2), we calculate the lifetime of $B^2\Sigma^+$ and $A^2\Pi$ state. For $v' = 0$ vibrational state of $B^2\Sigma^+$, the lifetime is computed to be 68.2 ns, which is in very good agreement with experimental measurement of (66 ± 2) ns,[12] demonstrating the reliability of our calculation. The lifetime of $v' = 0$ vibrational state of $A^2\Pi$ is calculated to be 8.3 ms, which agrees with theoretical result (4.1 ms)[26] in magnitude. The FCFs, Einstein coefficient $A_{v'v''}$, vibrational branching ratio $R_{v'v''}$, oscillator strength $f_{v'v''}$, transition energy $T_{v'v''}$, and transition wavelength λ for the $B^2\Sigma^+$–$X^2\Sigma^+$ transition are calculated and listed in Table 2. As shown in Table 2, the FCFs of $B^2\Sigma^+$–$X^2\Sigma^+$ transition are highly diagonal. The diagonal FCFs q_{00} and q_{11} are 0.972 and 0922, respectively, which are at least one order of magnitude larger than that of non-diagonal FCFs. Moreover, the diagonal Einstein coefficient $A_{v'v''}$ and vibrational branching ratio $R_{v'v''}$ demonstrate that the $B^2\Sigma^+$–$X^2\Sigma^+$ transition is dominant by those Δv $(v' - v'')$ =0 vibrational transitions. The A_{00}, R_{00}, and f_{00} are computed to be $1.43 \times 10^7 s^{-1}$, 0.976, and 3.22×10^{-2}, respectively, illuminating that the scattering probability to hot bands can be neglected.

Table 2. Spectroscopic quantities for $B^2\Sigma^+$–$X^2\Sigma^+$ transitions of SiO^+.

v''		$v'=0$	$v'=1$	$v'=2$	$v'=3$	$v'=4$	$v'=5$
0	$A_{v'v''}$	1.43×10^{7}	4.37×10^{5}	1.14×10^{4}	1.66×10^{2}	1.10	0.17
	$R_{v'v''(\%)}$	0.976	0.030				
	$R_{v'v''(\mathrm{exp.})}$[b]	0.97					
	$q_{v'v''}$		0.026	0.002			
	$T_{v'v''}$	25807	26917	28014	29098	30168	31225
	λ/nm	387.5	371.5	357.0	343.7	331.5	320.3
	$T_{v'v''(\mathrm{exp.})}$[b]	26030					
	$f_{v'v''}$	3.22×10^{-2}	9.20×10^{-4}	6.00×10^{-6}	2.48×10^{-8}	3.11×10^{-9}	3.66×10^{-10}
1	$A_{v'v''}$	3.41×10^{5}	1.35×10^{7}	8.14×10^{5}	3.41×10^{4}	7.92×10^{2}	9.97
	$R_{v'v''(\%)}$	0.023	0.925	0.056	0.003		
	$R_{v'v''(\mathrm{exp.})}$[b]	0.030					
	$q_{v'v''}$	0.027		0.082	0.002		
	$T_{v'v''}$	24655	25765	26862	27946	29016	30073
	$T_{v'v''(\mathrm{exp.})}$[b]	24870					
	$f_{v'v''}$	8.04×10^{-4}	2.96×10^{-2}	1.70×10^{-3}	1.39×10^{-5}	1.18×10^{-7}	1.16×10^{-8}
	λ/nm	405.6	388.1	372.3	357.8	344.6	332.5

[a]Note: Values of $R_{v'v''}$ and FCFs smaller than 0.001 are omitted in the table. [b]Ref. [12].

The laser cooling candidate of diatomic molecule requires a transition with two particular properties:[39,40] highly diagonal FCFs and a short radiative lifetime suitable for rapid laser cooling. These calculated results indicate that the $B^2\Sigma^+$–$X^2\Sigma^+$ transition of SiO^+ satisfies the two particular properties. According to our calculated spectroscopic quantities of $B^2\Sigma^+$–$X^2\Sigma^+$ transition of SiO^+, we propose a laser cooling scheme for the molecular ions by using two lasers at wavelengths around 400 nm. The wavelength of main pump laser is chosen to be 387.5 nm, which is near-resonance wavelength of the $B^2\Sigma^+$ ($v'=0$)–$X^2\Sigma^+$ ($v''=0$) transition. To suppress the unwanted vibrational branching loss, an additional laser ($\lambda=405.6$ nm) is used to repump the accumulated population at the $v''=1$ vibrational levels of the $X^2\Sigma^+$.

In Table 3, we summarize the dominant parameters of laser cooling of SiO^+, together with the corresponding parameters of other monohalides containing Group-IIA and Group-III A atoms which have already been suggested as molecular laser-cooling candidates in the previously theoretical investigations.[39,40] For comparison, the corresponding results for diatomic molecules that have been experimentally laser-cooled are also given in Table 3.[13,41,42] We can see that the q_{00} and lifetime of $B^2\Sigma^+$–$X^2\Sigma^+$ transition of SiO^+ are of the same order of experimentally laser-cooled molecules SrF, YO and CaF, illuminating the possibility of the proposed laser-cooling scheme of SiO^+.

Table 3. Comparison of q_{00}, R_{00}, λ_{00}, and τ between SiO^+ and other molecules suitable for laser cooling.

	SiO^+	$AlCl^+$[a]	$AlCl$[b]	SrF[c]	YO[d]	CaF[e]
q_{00}	0. 973	0.796	0.999	0.98	0.995	0.97
R_{00}	0.976		0.997			
λ_{00}	387.5	268	261.8	663.3	614	606
τ/ns	68.2	11.61	5	24	33	19

[a]Ref. [39], [b]Ref. [40], [c]Ref. [13], [d]Ref. [41], [e]Ref. [42].

3.3. Influence of spin–orbit coupling on spectroscopic properties

As shown in Fig. 1, the $B^2\Sigma^+$ state crosses ten electronic states ($1^2\Sigma^-$, $2^2\Sigma^-$, $2^2\Pi$, $1^2\Delta$, $a^4\Sigma^+$, $1^4\Sigma^-$, $2^4\Sigma^-$, $1^4\Pi$, $2^4\Pi$, and $1^4\Delta$) in a bond length range of $R=1.75$ Å–2.35 Å. Since the value of the SOC for each of $B^2\Sigma^+$–$2^2\Sigma^-$, $B^2\Sigma^+$–$1^2\Delta$, $B^2\Sigma^+$–$a^4\Sigma^+$, $B^2\Sigma^+$–$2^4\Sigma^-$, and $B^2\Sigma^+$–$1^4\Delta$ is close to zero, for clarity, none of the PECs of $2^2\Sigma^-$, $1^2\Delta$, $a^4\Sigma^+$, $2^4\Sigma^-$, and $1^4\Delta$ are not shown in the amplified view of the crossing regions of Fig. 2(a). The SO matrix elements between the $B^2\Sigma^+$ and $1^2\Sigma^-$, $2^2\Pi$, $1^4\Sigma^-$, $1^4\Pi$, $2^4\Pi$ are computed, which are used to qualitatively analyze the perturbation and predissociation of $B^2\Sigma^+$ caused by the SOC effect. The computed SO matrix elements each as a function of internuclear distance in the vicinity of the curve crossing regions are given in Fig. 2(b). The SO matrix element value of $B^2\Sigma^+$–$1^4\Pi$, $B^2\Sigma^+$–$1^4\Sigma^-$, $B^2\Sigma^+$–$2^2\Pi$, and $B^2\Sigma^+$–$1^2\Sigma^-$ are calculated to be 13, 30, 20, and 13 cm^{-1} at their crossing points, respectively, which can cause the the $v'>10$ vibrational levels of $B^2\Sigma^+$ to be perturbed.

Previous investigations show that the SOC effects are very important for spectroscopic properties of low-lying states, even when only light atoms are included.[43–46] By considering the SOC effects, different Λ–S states with common Ω components will be recombined and change the shape of PECs. Figure 3 only shows the PECs of the low-lying 15 Ω states. For clarity, the $\Omega=1/2$, and 3/2, 5/2, 7/2 are shown in Figs. 3(a) and 3(b), respectively. The calculated spin–orbit energy splitting for $^3P_1$–$^3P_2$ (O atom), $^3P_0$–$^3P_2$ (O atom) and $^2P_{3/2}$–$^2P_{1/2}$ (Si^+ ion) are 154, 231, and 290 cm^{-1}, respectively, which agree well with the existing experimental results of 158, 227, and 287 cm^{-1}.[47]

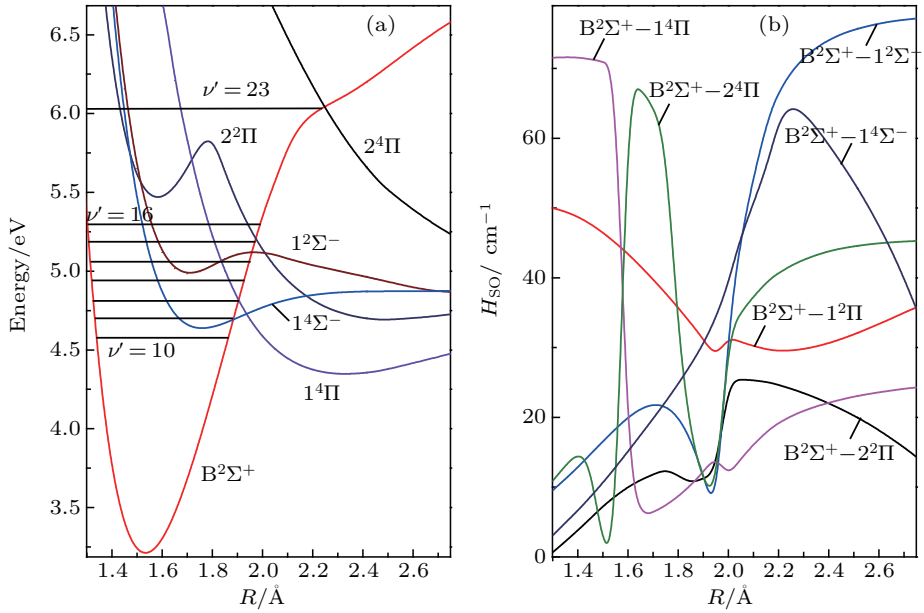


Fig. 2. (a) Magnified crossing regions together with vibrational levels of $B^2\Sigma^+$ and (b) corresponding SO matrix element values including $B^2\Sigma^+$.

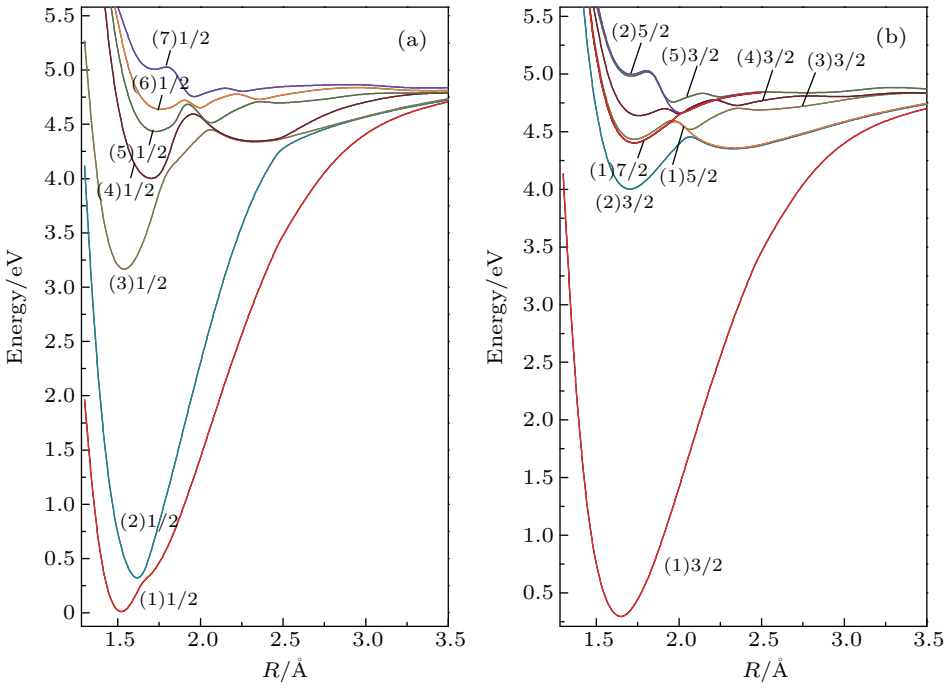


Fig. 3. Potential energy curves of the low lying Ω states of SiO^+: $\Omega = 1/2$ (a) and $\Omega = 3/2$, 5/2, and 7/2 (b).

Based on the PECs of the Ω states, the spectroscopic constants of SiO^+ molecular ion are numerically determined and presented in Table 4. For the (1)1/2 state, the calculated values of ω_e, B_e, and R_e agree with the experimental values,[24,48] but the spectroscopic constant $\omega_e x_e$ (12.8 cm^{-1}) is 5.9 cm^{-1} bigger than the experimental result 6.9 cm^{-1}.[48] The SOC effect causes $A^2\Pi$ splits into $A^2\Pi_{1/2}$ and $A^2\Pi_{3/2}$. Both $A^2\Pi$ and the ground state $X^2\Sigma^+$ have $\Omega = 1/2$ component, so the two states form an avoided crossing point around $R = 1.65$ Å. However, the $X^2\Sigma^+_{1/2}$ does not have $\Omega = 3/2$ component, so the (1)3/2 state ($A^2\Pi_{3/2}$ state) mainly originates from $A^2\Pi$. For the $A^2\Pi_{1/2}$ state, the T_e, ω_e, and R_e are computed to be 2422 cm^{-1}, 915 cm^{-1}, and 1.630 Å, which differ from the experimental results by less than 180 cm^{-1}, 29 cm^{-1}, and 0.006 Å, respectively.[17] The $B^2\Sigma^+$ state crosses the $1^4\Sigma^+$ state nearby $R = 1.75$ Å. Considering the SOC effects, the $B^2\Sigma^+$ and $1^4\Sigma^+$ states both have $\Omega = 1/2$ component, so the two states form an avoided crossing point around $R = 1.75$ Å. The T_e, ω_e, and $R_e$of $B^2\Sigma^+_{1/2}$ are computed to be 25454 cm^{-1}, 1140 cm^{-1}, and 1.535 Å, which are consistent with experimental results of 26016 cm^{-1}, 1137 cm^{-1}, and 1.545 Å, respectively.[17,22]

Table 4. Spectroscopic constants of bound Ω states of SiO^+.

State		T_e/cm^{-1}	ω_e/cm^{-1}	$\omega_e x_e$/cm^{-1}	B_e/cm^{-1}	R_e/Å
$X^2\Sigma^+_{1/2}$		0	1165	12.8	0.7192	1.518
	expt.[a]				0.7178	1.519
	expt.[b]		1120			1.512
	expt.[c]		1164		0.71762	
	expt.[d]				0.7325	
	expt.[e]		1162	6.9	0.72055	1.516
	Calc.[f]		1120			1.543
$A^2\Pi_{1/2}$		2422	915	3.2	0.6198	1.630
	expt.[b]	887	1030			1.645
	expt.[e]	2242	944	5.0	0.6189	1.636
	Calc.[f]	810	922			1.655
(3)1/2		25454	1140	9.3	0.7024	1.535
	expt.[a]				0.7103	1.527
	expt.[b]	25740	1180			1.545
	expt.[c]	26017	1138		0.71076	
	expt.[e]	26016	1137	6.9	0.71302	
(4)1/2	inner	32281	886	–12.8	0.5714	1.709
	Calc.[f]	30492	670			1.727
	outer	35103	336	3.2	0.3041	2.329
(5)1/2	inner	35774	564	–43.8	0.5536	1.727
	outer	36355	684	51.7	0.3949	2.059
(6)1/2		37446	$dG_{1/2} = 557$		$B_0 = 0.5301$	1.753
(7)1/2		40398				1.716
(1)3/2		2336	943	6.2	0.6107	1.649
	Calc.[f]	781	921			1.655
(2)3/2	inner	32282	740	15.0	0.5737	1.700
	Calc.[f]	30490	670			1.727
	outer	35156	270	3.1	0.3058	2.329
(3)3/2	inner	35774	646	25.6	0.5585	1.727
	outer	36407	617	38.5	0.3891	2.0603
(4)3/2	inner	37450	$dG_{1/2} = 538$		$B_0 = 0.5228$	1.754
	outer	38154	$dG_{1/2} = 582$		$B_0 = 0.2890$	2.350
(5)3/2		40179				1.707
(1)5/2	inner	35516	660	26.7	0.5590	1.727
	outer	35211	265	3.3	0.3056	2.328
(2)5/2	inner	40317				1.708
	outer	37607				2.002
(1)7/2		35513	679	29.8	0.5580	1.727

[a]Ref. [36]. [b]Ref. [22]. [c] Ref. [37]. [d]Ref. [38]. [e]Ref. [17]. [f]Ref. [26].

3.4. Ionization energy of SiO

To determine the ionization process of SiO, the PECs of the ground state $X^1\Sigma^+$ for the SiO molecule are calculated with the MRCI-F12 method through utilizing the same active space and basis set as those of SiO^+ calculation. The PECs of low-lying states of SiO and SiO^+ are plotted in Fig. 4, and these PECs are given by energy with respect to the minimum energy point of the $X^1\Sigma^+$ of SiO molecule. On the basis of the calculated PEC of the $X^1\Sigma^+$ of SiO, the ω_e and R_e are computed to be 1.514 Å and 1228 cm^{-1}, which are in good agreement with experimental values of 1.5097 Å and 1241.55 cm^{-1}.[36] Utilizing the vibrational wave function of low-lying states of SiO^+ and SiO, the FCFs between the $v = 0$ state of the $X^1\Sigma^+$ and vibrational states of the $X^2\Sigma^+$ are calculated. The FCFs' variations with ionization energy are presented in Fig. 5. As shown in Fig. 5, the vertical ionization energy of $X^2\Sigma^+$ is 11.5 eV, which is in reasonable agreement with experimental value of 11.61 eV.[22] As for the excited states $A^2\Pi$ and $B^2\Sigma^+$ of SiO^+, the vertical ionization energy values are calculated to be 12.1 eV and 14.7 eV, respectively, which are about 0.1 eV smaller than previous measurements of 12.19 eV and 14.80 eV.[22] As shown in Fig. 4, the equilibrium distance of the $X^2\Sigma^+$ and $B^2\Sigma^+$ states of SiO^+ are very similar to that of the $X^1\Sigma^+$ state of SiO, so the FCFs of $X^1\Sigma^+$–$X^2\Sigma^+$ and $X^1\Sigma^+$–$B^2\Sigma^+$ transitions are highly diagonal, and the q_{00} of the two transitions in Fig. 5 are both larger than 0.9. The equilibrium distance of the $A^2\Pi$ is 0.14 Å larger than that of the $X^1\Sigma^+$, so the vertical ionization process of $X^1\Sigma^+$–$A^2\Pi$ corresponds to the SiO^+ ($A^2\Pi$, $v^+ = 3$)+e$^-$ ← SiO ($X^1\Sigma^+$, $v = 0$)+$h\nu$ transition. The vertical ionization energy of $a^4\Sigma^+$ is computed to be 16.1 eV, corresponding to SiO^+ ($a^4\Sigma^+$, $v^+ = 7$)+e$^-$ ← SiO ($X^1\Sigma^+$, $v = 0$)+$h\nu$ transition. Since the equilibrium distance of the $X^2\Sigma^+$ and $B^2\Sigma^+$ states of SiO^+ are very close to that of the $X^1\Sigma^+$ state of SiO, the vertical ionization process of $X^2\Sigma^+$ (SiO^+) ← $X^1\Sigma^+$ (SiO) and $B^2\Sigma^+$ (SiO^+) ← $X^1\Sigma^+$ (SiO) are favorable, as compared with that of $A^2\Pi$ (SiO^+) ← $X^1\Sigma^+$ (SiO) and $a^4\Sigma^+$ (SiO^+) ← $X^1\Sigma^+$ (SiO).

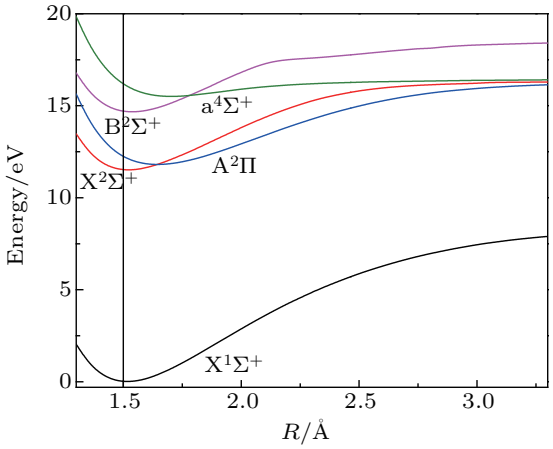


Fig. 4. MRCI-F12+Q potential energy curves of $X^2\Sigma^+$, $A^2\Pi$, $B^2\Sigma^+$, $a^4\Sigma^+$ states of SiO^+ and $X^1\Sigma^+$ state of SiO.

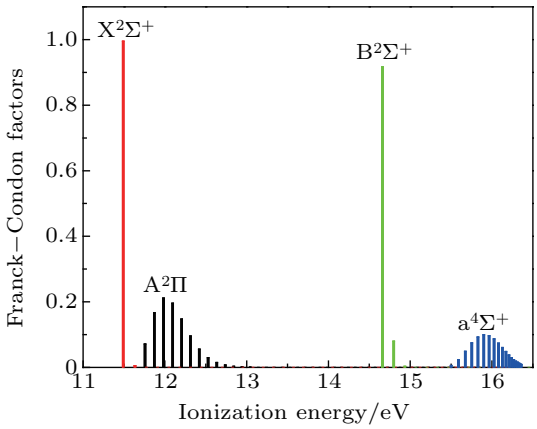


Fig. 5. Franck–Condon factors of transition between $X^1\Sigma^+$ state of SiO and $X^2\Sigma^+$, $A^2\Pi$, $B^2\Sigma^+$, $a^4\Sigma^+$ states of SiO^+ relative to ionization energy.

4. Conclusions

The electronic structures of low-lying states for SiO^+ are studied by the MRCI-F12 method with cc-pVQZ-F12 basis set. It can be seen from the calculated PECs that the $B^2\Sigma^+$ state crosses $1^4\Pi$, $1^4\Sigma^-$, $2^2\Pi$, $1^2\Sigma^-$, $2^4\Pi$ states in a internuclear distance range of 1.88 Å–2.25 Å. The calculated SO matrix between $B^2\Sigma^+$ state and these states are in a range of 13 cm^{-1}–30 cm^{-1} around the crossing points. With the help of the calculated SO matrices including $B^2\Sigma^+$ state, the predissociation mechanism of $B^2\Sigma^+$ state is explained in detail. On the basis of the calculated vibrational level and transition dipole moments, the radiative lifetimes of low-lying vibrational levels of $B^2\Sigma^+$ are computed, which are consistent with the most recent experimental results. Our calculations indicate that the FCFs and vibrational branching ratios of $B^2\Sigma^+$–$X^2\Sigma^+$ transition are highly diagonal, and the radiative lifetime of $B^2\Sigma^+$ is short. We propose a laser cooling scheme of SiO^+ that employs the $B^2\Sigma^+$–$X^2\Sigma^+$ transition. The vertical ionization energy values from SiO ($X^1\Sigma^+$) to SiO^+ ($X^2\Sigma^+$, $A^2\Pi$ and $B^2\Sigma^+$) agree with the previous experimental results. The present theoretical investigations will provide an in-depth understanding of the structure and spectroscopic properties of the SiO/SiO^+.

Acknowledgment

We thank the High Performance Computing Center of Qiqihar University for supercomputing time.

References

[1] Scalo J M and Slavsky D B 1980 *Astrophys. J.* **239** L73
[2] Clegg R E S, IJzendoorn V, J L and Allamandola L J 1983 *Mot. Not. R. Astr. Soc.* **203** 125
[3] Turner J L and Dalgarno A 1977 *Astrophys. J.* **213** 386
[4] Millar T J 1980 *Astrophys. Space Sci.* **72** 509
[5] Prasad S S and Huntress W T 1980 *Astrophys. J. Suppl. S.* **43** 1
[6] Herbst E, Millar T J, Wlodek S and Bohme D K 1989 *Astron. Astrophys.* **222** 205
[7] Tarafdar S P and Dalgarno A 1990 *Astron. Astrophys.* **232** 239
[8] Langer W D and Glassgold A E 1990 *Astrophys. J.* **352** 123
[9] Bauschlicher C W 2016 *Chem. Phys. Lett.* **658** 76
[10] Hartquist T W, Dalgarno A and Oppenheimer M 1980 *Astrophys. J.* **236** 182
[11] Neufeld D A and Dalgarno A 1989 *Astrophys. J.* **344** 251
[12] Stollenwerk P R, Odom B C, Kokkin D L and Steimle T 2017 *J. Mol. Spectrosc.* **332** 26
[13] Shuman E S, Barry J F and DeMille D 2010 *Nature* **467** 820
[14] Yzombard P, Hamamda M, Gerber S, Doser M and Comparat D 2015 *Phys. Rev. Lett.* **114** 213001
[15] Hamamda M, Pillet P, Lignier H and Comparat D 2015 *J. Phys. B: At. Mol. Opt. Phys.* **48** 182001
[16] Collaboration T A, Baron J, Campbell W C, DeMille D, Doyle J M, Gabrielse G, Gurevich Y V, Hess P W, Hutzler N R, Kirilov E, Kozyryev I, O'Leary B R, Panda C D, Parsons M F, Petrik E S, Spaun B, Vutha A C and West A D 2014 *Science* **343** 269
[17] Cameron R, Scholl T J, Zhang L, Holt R A and Rosner S D 1995 *J. Mol. Spectrosc.* **169** 364
[18] Scholl T J, Cameron R, Rosner S D and Holt R A 1995 *Phys. Rev. A* **51** 2014
[19] Scholl T J, Cameron R, Rosner S D and Holt R A 1995 *Can. J. Phys.* **73** 101
[20] Rosner S D, Cameron R, Scholl T J and Holt R A 1998 *J. Mol. Spectrosc.* **189** 83
[21] Zhang L, Cameron R, Holt R A, Scholl T J and Rosner S D 1993 *Astrophys. J.* **418** 307
[22] Colbourn E A, Dyke J M, Lee E P F, Morris A and Trickle I R 1978 *Mol. Phys.* **35** 873
[23] Werner H J, Rosmus P and Grimm M 1982 *Chem. Phys.* **73** 169
[24] Cai Z L and François J P 1999 *J. Mol. Spectrosc.* **197** 12
[25] Nguyen J H V and Odom B 2011 *Phys. Rev. A* **83** 053404
[26] Chattopadhyaya S, Chattopadhyay A and Das K K 2003 *J. Mol. Struc. Theochem.* **639** 177
[27] Werner H J, Knowles P J, Knizia G, *et al.* 2012 MOLPRO: a Package of *ab initio* Programs
[28] Peterson K A, Adler T B and Werner H J 2008 *J. Chem. Phys.* **128** 084102
[29] Knowles P J and Werner H J 1985 *Chem. Phys. Lett.* **115** 259
[30] Werner H J and Knowles P J 1985 *J. Chem. Phys.* **82** 5053
[31] Shiozaki T, Knizia G and Werner H J 2011 *J. Chem. Phys.* **134** 034113
[32] Balasubramanian K 1990 *Chem. Rev.* **90** 93
[33] Alekseyev A B, Liebermann H P, Lingott R M, Bludský O, Buenker R J 1998 *J. Chem. Phys.* **108** 7695
[34] Berning A, Schweizer M, Werner H J, Knowles P J and Palmieri P 2000 *Mol. Phys.* **98** 1823
[35] Le Roy R J 2002 LEVEL 7.5: *a Computer Program for Solving the Radial Schröinger Equation for Bound and Quasibound Levels* (University of Waterloo, Chemical Physics Research Report CP-655)
[36] Huber K P and Herzberg G 1979 *Molecular Spectra and Molecular Structure IV, Constants of Diatomic Molecules* (New York: Van Nostrand-Reinhold)
[37] Ghosh S N, Van der Linde J and Verma R D 1979 *J. Mol. Spectrosc.* **75** 169
[38] Nagaraj S and Verma R D 1968 *Can. J. Phys.* **46** 1597
[39] Kang S Y, Kuang F G, Jiang G, Li D B, Luo Y, Hui P F, Wang L P, Hu W Q and Shao Y C 2017 *J. Phys. B: At. Mol. Opt. Phys.* **50** 105103
[40] Wan M, Di Y, Jin C, Wang F, Yang Y, You Y and Shao J 2016 *J. Chem. Phys.* **145** 024309
[41] Hummon M T, Yeo M, Stuhl B K, Collopy A L, Xia Y and Ye J 2013 *Phys. Rev. Lett.* **110** 143001
[42] Truppe S, Williams H J, Hambach M, Caldwell L, Fitch N J, Hinds E A, Sauer B E and Tarbutt M R 2017 *Nat. Phys.* **13** 1173
[43] Sun E P, Ren T Q, Liu Q X, Quan M, Zhang J J, Xu H F and Yan B 2016 *Chin. Phys. Lett.* **33** 023101
[44] Ibraguimova L B and Minaev B F 2016 *Opt. Spectrosc.* **120** 345
[45] Cao J J, Gong T, Li Z H, Ji Z H, Zhao Y T, Xiao L T and Jia S T 2018 *Chin. Phys. Lett.* **35** 103301
[46] Wu D L, Tan B, Zeng X F, Wan H J, Xie A D, Yan B and Ding D J 2016 *Chin. Phys. Lett.* **33** 63102
[47] Moore C E 1971 *Atomic Energy Levels* (Washington, DC: National Bureau of Standard)
[48] Cameron R, Scholl T J, Zhang L, Holt R A and Rosner S D 1995 *J. Mol. Spectrosc.* **169** 352